Atmos. Chem. Phys. Discuss., doi:10.5194/acp-2016-426, 2016
Manuscript under review for journal Atmos. Chem. Phys.
Published: 27 June 2016

Atmospheric Chemistry and Physics Discussions

Chemistry-climate interactions of aerosol nitrate from lightning

Tost H.[1]

[1]Institute for Atmospheric Physics, Johannes Gutenberg University Mainz, Germany

Correspondence to: H. Tost (tosth@uni-mainz.de)

Abstract. Lightning represents one of the dominant emission source for NO_x in the troposphere. The direct release of oxidised nitrogen in the upper troposphere does not only affect ozone formation, but also chemical and microphysical properties of aerosol particles in this region. This study investigates the direct impact of LNO_x emissions on upper tropospheric nitrate using a global chemistry climate model. The simulation results show a substantial influence of the lightning emissions on the mixing ratios of nitrate aerosol in the upper troposphere of more than 50%. In addition to the impact on nitrate, lightning substantially affects the oxidising capacity of the atmosphere with substantial implications for gas phase sulphate formation and new particle formation in the upper troposphere. In conjunction with the condensation of nitrates, substantial differences in the aerosol size distribution occur in the upper troposphere as a consequence of lightning. This has implications for the extinction properties of the aerosol particles and for the cloud optical properties. While the extinction is generally slightly enhanced due to the LNO_x emissions, the response of the clouds is ambiguous due to compensating effects in both liquid and ice clouds. Resulting shortwave flux perturbations are of $\sim -100 mW/m^2$, but an uncertainty range of almost 50% has to be defined due to the large internal variability of the system and the uncertainties in the multitude of involved processes.

1 Introduction

Lightning is one of most energetic phenomenon in the Earth atmosphere. Due to the tremendous electricity, the associated temperatures allow for breaking up the stable molecular nitrogen compounds into fragments which partly recombine to nitrogen oxides (Schumann and Huntrieser, 2007). Hence lightning represents a natural atmospheric emission source for NO_x, in addition to the anthropogenic sources from industry, energy production, traffic and agriculture (e.g., Jaegle et al., 2005). Furthermore, biomass burning contributes significantly to the total NO_x emissions (e.g., van der

Atmos. Chem. Phys. Discuss., doi:10.5194/acp-2016-426, 2016
Manuscript under review for journal Atmos. Chem. Phys.
Published: 27 June 2016

Atmospheric Chemistry and Physics Discussions

Werf et al., 2010). The global lightning NO_x production has been estimated to range between 2 and 8 Tg N/yr (Schumann and Huntrieser, 2007), hence being in a similar order of magnitude as the soil emissions (e.g., Steinkamp and Lawrence, 2011), which represent an additional important natural contribution to the total oxidised nitrogen in the atmosphere. In contrast to the other sources (with the exception of aircraft emissions), LNO_x represents an upper tropospheric source. Due to a different chemical composition and chemical reactivity compared to the boundary layer, chemical conversion into HNO_3 is relatively efficient and most important is not subject to fast removal by dry deposition. Once nitric acid is formed this can condense on existing aerosol particles, mostly thermodynamically stabilised by ammonium (NH_4^+), forming ammoniumnitrate (NH_4NO_3). However, this aerosol species is considered semi-volatile such that in the lowermost atmosphere a substantial part of nitrate re-evaporates (e.g., Stelson et al., 1979). However, due to the lower temperatures in the upper troposphere, NH_4NO_3 is thermally stabilised, and remains mostly in the aerosol phase. However, the total amount of nitrate aerosol does not only depend on the available nitric acid, but also neutralising cations, i.e. mostly ammonium. Furthermore, the condensation rate of nitric acid forming nitrates also depends on the available aerosol concentration, as well as competition for neutralising compounds with e.g. sulphate ions.

Being a component of the mixture of aerosol particles, the nitrate aerosol from lightning can also influence atmospheric radiation via the direct and indirect aerosol effects by a multitude of pathways. First, nitrate contributes to water uptake increasing ambient aerosol size at a given relative humidity. Both the particulate nitrate mass as well as the additional aerosol water enhance the radiative extinction properties of the particle and can even alter the single scattering albedo influencing the direct aerosol effect of nitrate particles (e.g., Adams et al., 2001).

Additionally, the overall chemical composition of the aerosol is modified by nitrate from lightning such that the cloud condensation nuclei (CCN) or ice nuclei (IN) efficiency of the particles changes with implications for the indirect aerosol effects. Consequently, the indirect effect should be considered a competition between the formation of additional CCN (e.g., Makkonen et al., 2012) by the nitrate and a potential deactivation of IN for contact or deposition freezing by providing a hygroscopic coating. Immersion freezing is only affected to a minor degree via the concentration of the solutions and hence freezing point modifications.

Currently, only few global aerosol chemistry climate models can realistically simulate aerosol nitrate and its implications for the direct and partially also indirect aerosol effect due to the complex chemical interactions and the semivolatility (e.g., Jacobson, 2001; Adams et al., 2001; Bauer et al., 2007; Bellouin et al., 2011; Xu and Penner, 2012; Makkonen et al., 2012). Usually, the effect of nitrates is determined from *annihilation studies*, i.e. the effect of nitrates is completely ignored. However, this might have implications for the overall aerosol chemical composition and size distribution such that these effects are mixed with the pure impacts of nitrate. Instead of a total *annihilation sce-*

Atmos. Chem. Phys. Discuss., doi:10.5194/acp-2016-426, 2016
Manuscript under review for journal Atmos. Chem. Phys.
Published: 27 June 2016

Atmospheric Chemistry and Physics Discussions

nario, this study investigates the omission of only a fraction of the aerosol nitrate, which originates from the lightning NO_x emissions. According to our knowledge, the resulting climate impacts from lightning caused by particulate nitrate have not yet been quantified with a comprehensive chemistry climate model.

2 Model description

2.1 The EMAC modelling system

This study applies the ECHAM5/MESSy Atmospheric Chemistry (EMAC) model, which is a numerical chemistry and climate simulation system that includes sub-models describing tropospheric and middle atmosphere processes and their interaction with oceans, land and human influences (Jöckel et al., 2010). It uses the second version of the Modular Earth Submodel System (MESSy2) (Jöckel et al., 2005) to link multi-institutional computer codes. The core atmospheric model is the 5th generation European Centre Hamburg general circulation model (ECHAM5, Roeckner et al., 2006). For the present study we applied EMAC (ECHAM5 version 5.3.02, MESSy version 2.50) in the T42L31-resolution, i.e. with a spherical truncation of T42 (corresponding to a quadratic Gaussian grid of approx. 2.8 by 2.8 degrees in latitude and longitude) with 31 vertical hybrid pressure levels up to 10 hPa. The applied model setup comprised the submodels for radiation, convection, large-scale clouds and condensation and the budget (source, transport and loss processes) of chemical compounds in the gas and aerosol phase.

2.2 Aerosol climate processes within EMAC

To simulate the relevant processes mentioned above and sketched in Fig. 1, we employed the lightning NOx emissions scheme by Price and Rind (1992). This scheme uses convective cloud top height as simulated by the convection scheme (Tiedtke, 1989). Even though such a combination of two parameterisations is subject to large uncertainties we have shown in the past, that this special combination is relatively robust and able to provide relatively realistic lightning distributions compared to satellite data from the LIS/OTD sensors (Tost et al., 2007). The emitted NO_x is subject to gas phase chemical transformations which are calculated with the help of the chemical model MECCA (Sander et al., 2011). The resulting nitric acid (HNO_3) can subsequently partition into the aerosol phase. The corresponding aerosol processes are simulated with the GMXE aerosol submodel (Pringle et al., 2010; Tost and Pringle, 2012) taking both the gas-aerosol phase partitioning and the interactions with other chemical compounds as well as the microphysical properties of the aerosol particles into account. The gas-aerosol phase partitioning of inorganic semivolatile compounds is calculated by the ISORROPIA2 model (Fountoukis and Nenes, 2007), which is part of the GMXE aerosol scheme. The aerosol particles are discretised in 4 lognormal size categories, and for the larger three modes a distinction is done between internally mixed hydrophilic particles and externally mixed hydropho-

Atmos. Chem. Phys. Discuss., doi:10.5194/acp-2016-426, 2016
Manuscript under review for journal Atmos. Chem. Phys.
Published: 27 June 2016

Atmospheric Chemistry and Physics Discussions

bic particles resulting overall in 7 lognormal modes. Additional anthropogenic and natural emissions except for lightning are simulated with the submodels ONEMIS, OFFEMIS and TNUDGE (Kerkweg et al., 2006b) submodels, providing sources for other primary and secondary aerosol particles. Physical loss processes (dry and wet deposition, additionally sedimentation for aerosol processes) are explicitly considered in the schemes DRYDEP, SCAV and SEDI (Kerkweg et al., 2006a; Tost et al., 2006).

To consider aerosol radiation interactions the prognostic aerosol mass and number concentrations (including aerosol water) are used in lookup tables from Mie calculations precalculated with the LIBRADTRAN (Mayer and Kylling, 2005) to determine the radiative properties of the atmospheric aerosol (extinction, single scattering albedo, asymmetry parameter) as described in detail in Pozzer et al. (2012); de Meij et al. (2012) and Dietmüller et al. (2016). These parameters are explicitly considered in the radiation scheme native to ECHAM5 (Roeckner et al., 2003) replacing the aerosol climatology by Tanre et al. (1984) as described in Dietmüller et al. (2016). For the treatment of indirect aerosol effects, we have implemented a two moment cloud microphysics scheme (Lohmann and Hoose, 2009; Lohmann et al., 2010). The activation of aerosols is calculated with the scheme of Abdul-Razzak and Ghan (2000), which has been adapted to the simulated aerosol types. Furthermore, the interactions of aerosols in the homogeneous and heterogeneous freezing processes (Kärcher et al., 2006) are considered, including an adaption to the more comprehensive chemical composition of the aerosol simulated with GMXE. To investigate the sensitivity of the climate impacts of aerosol particles influenced by lightning caused by aerosol cloud interactions (ACI), a second set of simulations has been performed using a modified activation scheme based on a combination of the work of Abdul-Razzak and Ghan (2000) and Petters and Kreidenweis (2007), as described in detail by Chang et al. (2014). The set of simulations using the Abdul-Razzak and Ghan (2000) aerosol activation scheme will afterwards be abbreviated with ARG, for the other set of simulations following Chang et al. (2014) the KK (i.e. kappa-koehler) acronym will be used.

Both schemes include the effects of nitrate, but different approaches are followed to calculate the critical supersaturation: the ARG scheme uses parameters for the osmotic coefficient and dissociation of nitrate in the solution (which are more uncertain than for $(NH_4)_2SO4$), whereas the KK approach uses a volume weighted κ to determine the total aerosol water uptake and hence cloud formation potential. The two approaches are therefore merely a different representation of the Raoult effect in the cloud activation.

2.3 Simulation Setup

We performed decadal simulations including all feedback mechanisms with the EMAC model for present day and preindustrial conditions. Sea surface temperatures are prescribed by a climatology from the AMIPII database for all model configurations. To determine the effects of aerosols caused by lightning two simulations are performed for each scenario, one with and one without LNO_x

Atmos. Chem. Phys. Discuss., doi:10.5194/acp-2016-426, 2016
Manuscript under review for journal Atmos. Chem. Phys.
Published: 27 June 2016

Atmospheric Chemistry and Physics Discussions

emissions. Even though this annihilation scenario potentially cannot capture some compensation effects, we choose this approach due to the expected lower signal to noise ratio. Furthermore, as there is nitrate from anthropogenic, biomass burning and soil sources, there is no complete annihilation of all nitrate. For the present day scenario we applied emissions from the ACCMIP emission inventory (Lamarque et al., 2010) for trace gases and aerosol emissions from the AEROCOM (Dentener et al., 2006) experiment, for preindustrial conditions we followed the AEROCOM (Dentener et al., 2006) recommendation for preindustrial conditions. Biomass burning is included using the GFED data (van der Werf et al., 2010), as well as a compilation for preindustrial biomass burning. Note, that we applied prescribed aerosol emissions for dust and sea salt, not including a potential feedback of a changed circulation (wind speed and wind patterns) on aerosol sources. The model simulations have been initialised with results from previous experiments eliminating spin-up effects. Due to the comprehensive feedback mechanisms we refrain from comparing individual years of the simulations, but focus on the decadal mean values and distributions.

3 Results

3.1 Lightning and associated emissions

To estimate the effects of lightning and associated emissions, we have analysed the distribution of NO_x emissions from lightning. Fig. 2 depicts in a 3D visualisation the temporal mean emitted LNO_x for the present day scenario.

The magnitude of the LNO_x emissions is displayed as an isosurface of $1 \cdot 10^{-16}$ kg/(m^3 s). A second isosurface of $3 \cdot 10^{-16}$ kg/(m^3 s), which is visible as a darker shading embedded in the first isosurface, shows that the dominant emissions take place in the upper part of the LNO_x plume. This is a consequence of the fact that the vertical emissions redistribution follows a C-shape profile according to Pickering et al. (1998), leading to enhanced emissions in the upper section of the plume.

The colour coding of the isosurface displays the total aerosol nitrate mixing ratio (in mol/mol), depicting the amount of aerosol nitrate present at the emission peaks. Furthermore, the gray shaded isosurface visualises an isosurface of 0.1 ppb$_v$ of aerosol nitrate. This shows that even though the higher aerosol nitrate concentrations are located in the lower troposphere, also enhanced mixing ratios of particulate nitrate can be found in the upper troposphere, partially concurring with the LNO_X emissions. The higher NO_3^- mixing ratios closer to the surface can be explained by the higher anthropogenic NO_x emissions as well as sources for neutralising cations such as NH_4^+.

The coloured map at the bottom of Fig. 2 depicts the mean flash frequency per second, which is relatively well confined to the tropical continents. Consequently, also the LNO_x emissions are co-located over the same regions.

The total LNO_x emissions are 5.95 Tg N/yr with a 1σ-variability of 0.03 Tg N/yr over the simulated decade in the present day scenario (ARG). Note that the seasonal variability is substantially

Atmos. Chem. Phys. Discuss., doi:10.5194/acp-2016-426, 2016
Manuscript under review for journal Atmos. Chem. Phys.
Published: 27 June 2016

Atmospheric Chemistry and Physics Discussions

larger. In the preindustrial scenario total LNO_x emissions of 6.12 ± 0.03 Tg N/yr are simulated. More than 80% of the emitted LNO_x is placed above 500 hPa altitude in both scenarios. The difference between the two scenarios is a consequence of slightly different meteorological conditions which are caused by the feedback effects of the aerosol and cloud properties. For the KK scenario again the feedback slightly alters the emissions from lightning with 6.04 ± 0.03 and 6.16 ± 0.03 Tg N/yr for present day and preindustrial conditions, respectively, with also more than 80% of the emitted NO_x above 500hPa.

3.2 Tropospheric nitrate from lightning

3.2.1 Chemical budgets and distribution of oxidised nitrogen compounds

The emitted NO_x from lightning mixes with other NO_x molecules in the atmosphere forming HNO_3 mostly via the gas phase reaction of $NO_2 + OH \rightarrow HNO_3$. The LNO_x emissions for the present day scenario result in $\sim 40\%$ higher nitric acid mixing ratios in the troposphere, and even up to $\sim 61\%$ between 500 hPa and the tropopause, compared to simulations without lightning NO_x emissions (see Tab. 1). Even though the enhancement effect for N_2O_5 is stronger in relative numbers, the overall mixing ratios for N_2O_5 are substantially smaller (almost two orders of magnitude) such that dinitrogenpentoxide plays a minor role for the highly oxidised nitrogen compounds in the troposphere.

During preindustrial times, this effect is even more amplified with $\sim 67\%$ and $\sim 76\%$ increases for HNO_3 in the total and upper troposphere, respectively. This stronger enhancement is due to the larger contribution of the LNO_x emissions compared to the total NO_x release, which is mostly from anthropogenic sources in present day conditions. Enhancements for N_2O_5 are of $\sim 80\%$, but also under these conditions N_2O_5 is a minor contributor to the total highly oxidised nitrogen tropospheric load (less than 5%).

The nitric acid molecules can condense on pre-existing aerosol particles forming NO_3^- ions in the deliquesced aerosol solution or solid NH_4NO_3 or $NaNO_3$ crystals. Tropospheric nitrate mixing ratios are typically a factor two to three lower compared to HNO_3. Nevertheless, the changes in upper tropospheric NO_3^- mixing ratios are globally averaged $\sim 32\%$. Fig. 3 shows isosurfaces of tropospheric nitrate concentration differences between the simulation with LNO_x emissions to the case without this source. The grey shaded isosurface depicts a 30% difference, the blue isosurface 45% differences and the red enclosed area 60% enhanced NO_3^- mixing ratios. Even though the maximum NO_3^- absolute differences occur down to the surface, the largest relative differences are apparent in the UT. Most of these differences are constrained to the tropics where the strongest LNO_x emissions are prevalent. However, the maxima in the differences are not co-located with the emission maxima (i.e. Central Africa, Amazonia and the maritime continent, see Fig. 2), but generally further downwind. This is a consequence of atmospheric transport during the time required for oxidation of NO_x to HNO_3 and subsequent partitioning into the aerosol phase.

Atmos. Chem. Phys. Discuss., doi:10.5194/acp-2016-426, 2016
Manuscript under review for journal Atmos. Chem. Phys.
Published: 27 June 2016

Atmospheric Chemistry and Physics Discussions

Additionally, the mean upper tropospheric column burden (500 hPa to the tropopause) in mg/m^2 is depicted by the coloured panel at the bottom of the plot. The turquoise isolines on this panel depict the 20%, 40% and 60% differences in the UT column burden between the simulations with and without LNO_x emissions.

A similar figure for preindustrial conditions can be found in the supplement. Due to the lower other sources of NO_x in the atmosphere, the importance of the LNO_X emissions is substantially increased. Therefore, the relative differences in NO_3^- are larger which can be seen from the extended areas included by the respective isosurfaces and the larger areas covered by the turquoise contour lines at the floor panel of the figure. The lower overall nitrate mixing ratios are obvious from the colour scale of the column nitrate which is almost an order of magnitude lower compared to present day conditions.

The tropospheric budget of the highly oxidised N compounds is summarised in Tab. 1, including the relative importance of the LNO_x emissions. For present day conditions, the particulate nitrate contribution to the total N(V) is $\sim$ 25%, whereas in the upper troposphere it is only $\sim$ 13%. For preindustrial conditions a lower contribution of particulate nitrate to the total N(V) load with 22% for the whole and 9% for the upper troposphere is simulated. The lower contribution for the preindustrial conditions can be mostly attributed to lower NH_3 emissions and consequently less NH_4^+ ions to neutralise and thermodynamically stabilise available aerosol nitrate.

The neglect of the LNO_x emissions leads to a shift in the contribution of the particulate phase to the total N(V). Under these conditions 33% of the N(V) is in the form of particulate NO_3^- for the whole troposphere, whereas for the UT the fraction is higher than 21%. This is a consequence of the reduced available N(V), but a similar amount of neutralising cations, i.e. mostly NH_4^+. For preindustrial conditions this enhancement of the particulate phase is even stronger to $\sim$ 34% for the whole troposphere and 17% for the UT.

The sensitivity simulations in the KK configuration result in almost identical values, (budget is shown in Tab. 1 of the supplement) depicting the fact that the description of cloud and cloud removal processes plays a minor role for the total budget of particulate nitrate in both model configurations.

The budget of the loss processes of N(V) compounds can be found in the supplement for both present day and preindustrial conditions.

3.2.2 Influences on other chemical species

The reduced NO_x burden in the simulation without lightning emissions has substantial impact on the concentrations of other species. As only a minor fraction of the total LNO_X emissions of $\sim$ 6 Tg N/yr are converted to N(V+) (e.g. 186 Gg N change in N(V) according to Tab. 1), the impact on ozone is comparable to previous studies (e.g., Labrador et al., 2005): the calculated values for tropospheric ozone are 362 Tg in the simulation without lightning and 444 Tg if lightning is included, which corresponds to a 22% increase in the tropospheric ozone burden. This effect is again very

Atmos. Chem. Phys. Discuss., doi:10.5194/acp-2016-426, 2016
Manuscript under review for journal Atmos. Chem. Phys.
Published: 27 June 2016

Atmospheric Chemistry and Physics Discussions

prominent in the upper troposphere, where the O_3 load increases from 195 to 248 Tg by LNO_x emissions, i.e. an increase of 27%. Driven by the location of most of the emissions, these effects mostly occur in the low latitudes. The resulting decrease in ozone in the zonal average resulting from neglecting lightning emissions is comparable to the findings of Grewe (2007). The change in the column burdens in the tropics also agrees with the results of Martin et al. (2002), both in the geographic patterns and the amplitude of the signal. Therefore concluding, the explicit consideration of the nitrate formation has no important impact on the tropospheric ozone distribution, such that the results of impact studies of lightning NO_x (such as e.g., Banerjee et al., 2014) do not have to be revised.

However, the OH concentrations and therefore the oxidation capacity of the atmosphere are also substantially influenced by lightning (Labrador et al., 2004). The effect on OH is displayed by a modification of the methane lifetime, as depicted in Tab. 2. The emissions of LNO_x are responsible for an increase of the tropospheric methane lifetime of ~ 1.7 to 1.9 years; however in the upper troposphere (above 500 hPa up to the tropopause) an increase of the CH_4 lifetime of almost 10 and 13.2 years for present and preindustrial conditions, respectively, corresponding to almost a halving of the oxidation capacity of the atmosphere.

This is especially relevant for the production of sulphate via the gas phase oxidation of SO_2, which substantially influences aerosol formation and aerosol composition in the upper troposphere. The sulphate burden for present day conditions decreases from 576 Gg S(VI) to 565 Gg. This is also prominent in the UT region, where instead of 74.6 Gg S(VI) only 70.2 Gg S are simulated. For preindustrial conditions a similar reduction in the sulphate load is calculated without LNO_x emissions despite the substantially lower total SO_2 emissions.

Particulate ammonium mixing ratios are only affected to a minor degree by the LNO_x emissions: for present day conditions the NH_4^+ burden slightly decreases without lightning emissions, but increases during preindustrial times. However, the changes in the atmospheric burden are lower than $\pm 5\%$. These changes can be explained by the of lower sulphate and nitrate burdens and effects of the oxidation capacity on gaseous ammonium concentrations. A significant change due to LNO_x emissions in the sulphate to bisulphate ratio is not simulated by the model despite the capabilities of the thermodynamic equilibrium model.

The KK simulations show a very similar behaviour in the burdens, the CH_4 lifetime and the changes induced by the omission of the LNO_x emissions, such that a detailed discussion is skipped here.

3.3 Aerosol microphysical effects

The influences of the chemical composition in the upper troposphere due to lightning are also reflected in the microphysical properties of the aerosol, which are described by the size distributions at various locations.

Atmos. Chem. Phys. Discuss., doi:10.5194/acp-2016-426, 2016
Manuscript under review for journal Atmos. Chem. Phys.
Published: 27 June 2016

Atmospheric Chemistry and Physics Discussions

The temporal mean size distributions of the aerosol particles for various regions (i.e. those regions covered by the plot on the map) are shown in Fig. 4 as a 2D plot with the horizontal axis depicting the ambient aerosol diameter and the vertical axis the pressure altitude; the colour coding displays the relative difference in aerosol number concentration [in $\%$] between the simulation with and without lightning. Furthermore, the absolute values of the size distribution [in cm^{-3}] are depicted by the contour lines. The figure shows the simulation results for the present day conditions (ARG case), for preindustrial conditions a similar figure can be found in the supplement.

Over the tropical continents in the upper troposphere enhanced nucleation mode particle numbers are simulated if lightning emissions are considered, which is a result of the enhanced S(VI) concentrations and consequently enhanced new particle formation. At approximately 10 nm diameter the particle number is smaller in case of $\mathrm{LNO_x}$ emissions, due to the interaction of enhanced coagulation and condensation on the enhanced particle concentrations. Also additional condensation on existing particles and enhanced coagulation with the small particles causes the reduction of particle numbers at $\sim$ 80 nm. For larger particles a slight reduction is found as a consequence of the more efficient coagulation (due to higher particle numbers in the small mode) versus the slower condensational growth. For the lower troposphere the picture is more ambiguous: in South America and Indonesia reduced nucleation takes place. However, the absolute particle concentrations are so low that this process is almost negligible, whereas in Central Africa enhanced new particle formation is caused by lightning emissions. For the larger particles the impact is rather small.

In the mid-latitudes relevant changes in the size distributions are only found in the Eastern US and China but little impact in Europe and Siberia. The first two regions are located slightly more southwards such that lightning frequencies are enhanced compared to the latter two regions (see bottom map of Fig. 2.

In the Southern Atlantic region the changes in the size distribution profile are relatively small, as lightning emissions play a minor role for the total particle concentration as well as for the oxidation capacity of the atmosphere and therefore sulphate formation. In the Central Pacific where enhanced nitrate concentrations are simulated in the upper troposphere (see Fig. 3), the changes in the aerosol size distribution are moderate with strongest signals in the middle troposphere (between 700 and 500 hPa). As lightning $\mathrm{NO_x}$ emissions are substantially smaller over the ocean, the oxidation capacity is affected to a minor degree; however nitrate and gaseous N(V) are transported downwind from the source region affecting the nitrate concentrations and particle numbers, mostly via coagulation.

For preindustrial conditions (see supplement) the simulation provides similar results from the tropics. However, in the mid-latitudes where a substantial reduction of other $\mathrm{NO_x}$ emissions is applied compared to the present day scenario the impact of lightning on the nitrogen budget as well as the size distribution becomes more important. Obviously, a similar pattern as for the tropical continents is simulated; however, due to the weaker $\mathrm{LNO_x}$ emissions in the mid-latitudes the effects are substantially smaller compared to the tropics.

Atmos. Chem. Phys. Discuss., doi:10.5194/acp-2016-426, 2016
Manuscript under review for journal Atmos. Chem. Phys.
Published: 27 June 2016

Atmospheric Chemistry and Physics Discussions

To analyse the impact of the LNO_x emissions on the aerosol water uptake, the mean growth factor (GF = ambient diameter / dry diameter) is compared. Using this parameter has the advantage, that - in contrast to e.g. the aerosol water content - it is independent of the aerosol size and number concentrations. The overall impact of lightning on the GF is relatively small: for present day conditions the nucleation and aitken mode depict a slight increase in the upper troposphere (up to 2%), whereas in the accumulation and coarse mode a decrease of up to -2% is simulated caused by LNO_x emissions. Closer to the surface the differences are even smaller and ambiguous in their sign.

For preindustrial conditions the results are similar in their distribution with a slightly increased amplitude (up to $\pm 5\%$). The sensitivity simulations *KK* are characterised by the same distribution and dependencies on the emissions by lightning. Corresponding figures can be found in the supplement.

3.4 Impacts on climate

3.4.1 Aerosol optical properties

As aerosol particles scatter and absorb solar and infrared radiation, the impact of the LNO_x emissions is investigated with the help of Fig. 5 for the ARG present day simulation. The floor panel depicts the annual mean aerosol optical depth (AOD) at 550 nm wavelength with maximum values in the dust emission regions (e.g. Northern Africa) and the anthropogenic pollution centers (e.g. Eastern China). The climatological global mean value with present day emissions is 0.122, which is close to the observations as derived from MODIS (e.g., Mao et al., 2014). The influence of the LNO_x emissions can be analysed with the help of the ceiling map in Fig. 5, which shows the percentage fractions of the changes in the simulated AOD. Globally a slight reduction to 0.121 can be found ($\sim 1\%$). However, in some regions even higher extinction is simulated in case of no nitrate formation from lightning, which is in contrast to the findings of Sect. 3.2.1, where no regions with enhanced nitrate have been simulated. These regions are mostly oceanic or remote with little direct impact by either lightning and primary emissions.

The zonal mean of the average extinction per km is provided in the rear panel of Fig. 5. Substantial extinction is simulated in the lower troposphere (below 700 hPa) with an additional enhancement of the optical depth between 20° and 50°N. The relative changes due to LNO_x are depicted in the front panel. The most substantial enhancement of aerosol extinction is simulated in the middle to upper troposphere in the tropics with zonal mean enhancements higher than 10%. In the uppermost troposphere also reductions in extinction are simulated as a consequence of neglecting the lightning emissions. Please note, that the stratospheric influences are masked in the zonal mean views as the stratospheric circulation and processes are not well resolved with this model configuration. Compared to the nitrate enhancements as analysed from Fig. 3, the maximum enhancement by LNO_x

Atmos. Chem. Phys. Discuss., doi:10.5194/acp-2016-426, 2016
Manuscript under review for journal Atmos. Chem. Phys.
Published: 27 June 2016

Atmospheric Chemistry and Physics Discussions

is located further downwards in the middle troposphere, i.e. between 400 and 600 hPa, whereas the strongest nitrate enhancement has been simulated between 200 and 400 hPa.

The isosurfaces depicting the regions of enhancements and reductions of extinction in Fig. 5 provide further information on their locations. The pale red depicts the $+10\%$ isosurface, whereas the embedded dark red regions mark an increase of the extinction due to $\mathrm{LNO_x}$ of more than $+20\%$. On the other hand the pale blue marks regions of a medium reduction (-10%) and dark blue regions (only at the tropopause) depict extinction reductions of more than 20%. The main enhancement of extinction by lighting emissions occur between 400 and 600 hPa over the tropical continents and slightly further downwind. This general pattern corresponds to the enhanced nitrate mixing ratios (c.f. Fig. 3), but is more restricted to the continents. In the extra-tropics an even higher extinction is simulated if no $\mathrm{LNO_x}$ emissions are considered. This is a consequence of the secondary effects caused by the emissions, i.e. the influence on sulphur oxidation via the oxidation capacity of the atmosphere and changes in the size distribution. Comparing the pattern correlation between the changes in nitrate and extinction a relatively low value is found ($R \approx 0.3$). However, the changes in sulphate and extinction show a higher correlation value of $R \approx 0.4$.

For preindustrial conditions the situation is quite comparable (see supplement), despite the intensive AOD signals in the regions with anthropogenic pollution, especially East Asia. The simulated global mean column AOD at 550 nm is 0.090. Consequently, the enhancement of the extinction between 20° and 50°N is less strong. The neglect of the lightning emissions results in a reduced column AOD in most regions, resulting in a global mean value of 0.089. A reduction in column AOD occurs only in regions of strong hydrophobic emissions (dust or BC) where the aerosol lifetime is reduced by a coating by nitrates and subsequent faster conversion from hydrophobic to hydrophilic categories, e.g. in the Northern part of the Saharan outflow or in Southern Africa. The extension of the $+10\%$ isosurface in the tropical upper troposphere is smaller, especially over Central Africa and the maritime continent. In contrast, over South America the enhancement of aerosol extinction caused by the $\mathrm{LNO_x}$ emission is even stronger. On the other hand, also slightly more reductions in extinction are simulated in the extra-tropics and mid-latitude upper troposphere, but they hardly exceed the -10% level.

Analysing the PDF of the differences in AOD between the simulation with and without lightning emissions (not shown) reveals that for present day conditions larger deviations occur more often compared to the preindustrial cases. The PDFs are almost symmetric, but show a slight shift towards enhanced extinction in the simulations including $\mathrm{LNO_x}$ emissions.

The sensitivity simulations with the alternative warm cloud activation scheme in general show a similar distribution of the aerosol extinction with the enhancement in the middle and upper tropical troposphere (see supplement). The global mean column AOD for present day conditions is slightly lower (0.120) and the reduction in case of no $\mathrm{LNO_x}$ emissions even further reduced ($\sim 0.5\%$). Strongest enhancement is found over the tropical continents, i.e. the regions with maximum light-

Atmos. Chem. Phys. Discuss., doi:10.5194/acp-2016-426, 2016
Manuscript under review for journal Atmos. Chem. Phys.
Published: 27 June 2016

ning activity, but most of the nitrate is simulated in the upper troposphere, whereas also in this configuration the extinction is enhanced in the middle to upper troposphere. For preindustrial conditions, the enhancement of the extinction by lightning is a bit stronger, but still small ($\sim 1\%$).

To analyse whether the contribution of scattering versus absorption is influenced by the LNO_x emissions, the single scattering albedo is compared in both model simulations. The zonal mean value changes by less than $\sim +1\%$ in the free troposphere and stratosphere, and is reduced by a maximum of $\sim -4\%$ in the boundary layer when lightning emissions are considered. Consequently, a change in the thermodynamic structure resulting from direct aerosol-radiation interactions is expected to be small.

3.4.2 Cloud properties

As cloud properties can be influenced indirectly by the LNO_x emissions three parameters are analysed to provide the causes for aerosol-cloud-radiation interactions. The cloud cover may hint at modifications of the cloud lifetime effect (Albrecht, 1989), whereas the combination of the liquid (ice) water content and the cloud droplet (ice crystal) numbers, which can also be expressed via the effective radii, can shed light onto the direct influence of the lightning emissions on the radiative properties of the clouds via the Twomey (1977) effect.

- Cloud cover:
  The cloud and precipitation cover changes only to a minor degree between the simulations with and without lightning for the present day scenario (ARG case). In the tropics the LNO_x emissions lead to a small increase in the mid troposphere cloud coverage of the Northern hemisphere, whereas the dipole pattern is compensated by reduced cloudiness in the Southern hemisphere. Apart from this only the polar latitudes show some significant changes in cloud coverage. Consequently, the impact of the cloud lifetime effect is expected to be small.

- Liquid / ice water content:
  The patterns for cloud water and cloud ice are characterised local dipole changes, but no significant modifications of the distribution of cloud water and ice, respectively. Only the tropical middle to upper troposphere of the Northern hemisphere shows an enhanced ice mixing ratio in the simulation with lightning emissions, which correlates to the increase in cloud coverage. However, the decrease in cloud coverage in the corresponding region in the Southern hemisphere is not accompanied by a substantial decrease in ice water. In the zonal average the increase is on the order of 10%.

- Cloud droplet / ice crystal numbers:
  Compared to the other two parameters, some substantial changes in cloud droplet and especially in crystal number are found as a consequence of the LNO_x emissions. For the present day scenario, in the troposphere between 650 and 400 hPa an increase in cloud droplets is

Atmos. Chem. Phys. Discuss., doi:10.5194/acp-2016-426, 2016
Manuscript under review for journal Atmos. Chem. Phys.
Published: 27 June 2016

Atmospheric Chemistry and Physics Discussions

simulated in case of active lightning emissions. Further North a decrease of cloud droplets between 900 and 600 hPa is calculated. Both are of approximately the same magnitude both in absolute and in relative terms and are a consequence of more hydrophilic particles due to nitrate coating and a reduction of lower tropospheric CCN due to reduction in lifetime and faster conversion from hydrophobic to hydrophilic conditions. For the ice crystal number the influence is even stronger: in the tropical upper troposphere the LNO_x emissions lead to an increase in the ice crystal number in a region where the highest ice crystal numbers are simulated. In the mid-latitudes a reduction of the ice crystal numbers is simulated in both hemispheres above 400 hPa. Both modifications are of the order of more than $\pm 20\%$. Due to the coarse temporal resolution of the data it is not possible to attribute the differences to a change in regime from homogeneous to heterogeneous freezing. Nevertheless, it is possible that locally this effect can occur and have a substantial influence on the ice crystal number concentration.

Analysing the effective radii with the help of Fig. 6, some of the effects on water mixing ratios and numbers compensate, whereas others positively amplify each other. This is both valid for liquid clouds in the lower and middle troposphere. For these clouds, the effective radii increase in the simulation with lightning in the polewards of 40° below 800 hPa and in the tropics (0° to 20°N) up to 400 hPa. For ice clouds the effective radii also increase in the same tropical latitude range between 600 and 200 hPa. Additionally, a decrease in effective radii of similar magnitude on the other side of the ITCZ is simulated. Also in the high latitudes the effective ice crystal size mostly increases in the simulation with LNO_x emissions, both in the upper troposphere as well as in the boundary layer.

For preindustrial conditions the response to the LNO_x emissions is comparable, but shows a slightly higher amplitude. Using the KK model configuration, which applies a different cloud droplet activation scheme, results in a lower sensitivity of the liquid droplet effective radius at elevated altitude for present day conditions. However, in the lower troposphere a similar strong signal is simulated, which leads to an increase of effective droplet radius in the tropical Southern hemisphere and a decrease in the Northern counterpart. For ice crystals, mostly a reduction of effective crystal size is simulated which is a consequence of the liquid droplet freezing. The effects for preindustrial conditions are similar, with even lower sensitivity of the low clouds on the lightning emissions.

In general, the regions with positive and negative effects in the effective droplet and crystal size show ambiguous signals, such that the impact on cloud radiative properties can only be addressed in conjunction with cloud coverage and the calculation of the radiative fluxes.

3.4.3 Radiative Fluxes

The combined effects of modifications in the aerosol extinction and the cloud optical properties lead to a modification of the shortwave and longwave radiation fluxes. In Fig. 7 the mean impact on the total sky shortwave flux is depicted in the upper panel. Shown are the differences in the SW flux

Atmos. Chem. Phys. Discuss., doi:10.5194/acp-2016-426, 2016
Manuscript under review for journal Atmos. Chem. Phys.
Published: 27 June 2016

Atmospheric Chemistry and Physics Discussions

at the top of the atmosphere between a simulation with and one without LNO_x emissions (ARG configuration). Despite the relatively large internal variability of the system, several regions show a statistical significant change in the TOA short wave flux (based on a t-test with 90% significance threshold on the annual mean data), which are marked by the hatched regions. However, the regions with increased or decreased fluxes are not directly co-located with the LNO_x emissions. Downwind of Central Africa an increased TOA short wave flux (corresponding to a heating) is simulated, whereas in Northern Amazonia and the maritime continent a decrease of the fluxes (corresponding to a cooling) is calculated. Also in the mid-latitude storm tracks mostly a slight increase in the fluxes is simulated, whereas over the tropical oceans the model suggests decreased fluxes. In the global mean the overall effect is determined as an enhanced backward reflection of the shortwave radiation of ~ -0.1 W/m^2 for all sky conditions. However, the time series of the global mean differences (depicted in the lower panel of Fig. 7) is characterised by large internal variability with both positive and negative differences. The clear sky fluxes show a substantially weaker signal with only ~ -0.05 W/m^2 and hardly any regions with statistical significance. Furthermore, the patterns of substantial changes are clearly separated from the regions where lightning is dominant (i.e. mid-latitudes versus tropical continents). Consequently, the clear sky signal is interpreted as statistical noise.

For preindustrial conditions (for a graph see supplement) the situation is comparable with a slightly increased amplitude of ~ -0.14 W/m^2 and a similar pattern distribution. The clear sky signal is almost negligible with ~ -0.01 W/m^2 and no statistical significance.

Considering both the temporal variability of the mean and the large spatial variability, the uncertainty in the total effect has to be considered as relatively large. Using the sensitivity simulations with the alternative cloud activation scheme reveals for both present day and preindustrial conditions a shortwave flux perturbation of ~ -0.06 W/m^2 again with no significant contribution from the clear sky fluxes.

To bring these numbers into context with the total shortwave flux disturbances from anthropogenic aerosols, simulation results with both cloud activation schemes and present day and preindustrial emission scenarios are intercompared (for figures see supplement). Both model configurations show a statistical significant cooling over the regions of dominant anthropogenic aerosol pollution (Eastern US, Europe, China) for both clear sky and all sky conditions. The clear sky disturbance is ~ -0.57 for the ARG and ~ -0.50 W/m^2 for the KK configurations. All sky fluxes change by ~ -1.62 for the ARG and ~ -1.42 W/m^2 for the KK simulation setups, respectively. The overall anthropogenic aerosol effect is relatively large in the simulations compared to the results published in the latest IPCC report (IPCC, 2013) and therefore an overestimated sensitivity to the aerosol disturbance by lightning NO_x nitrate cannot be ruled out completely.

Atmos. Chem. Phys. Discuss., doi:10.5194/acp-2016-426, 2016
Manuscript under review for journal Atmos. Chem. Phys.
Published: 27 June 2016

Atmospheric Chemistry and Physics Discussions

The effect on the longwave radiation via both aerosol extinction and cloud effects is relatively small. Especially, the clear sky flux disturbances are almost negligible, such that the total effect is dominated by ACI.

Consequently, as the differences between both cloud activation schemes indicate an uncertainty of almost 50% the quantitative estimate of -100 mW/m^2 should also be used with a comparable uncertainty range of 50 mW/m^2.

4 Conclusions

The overall impact of chemically produced aerosol nitrate from lightning NO_x emissions is analysed with a global chemistry climate model. Based on a total emission of 6 Tg N/yr, the contribution of LNO_x to the concentrations of upper tropospheric oxidised nitrogen by more than 57% for present day and 75% for preindustrial conditions. Given a sufficient amount of neutralising cations, especially NH_3 substantial amounts of aerosol nitrate are formed with the increases in the upper tropospheric burden exceeding 30% for present day and 50% for preindustrial conditions. Therefore, lightning is also a major contributor to the aerosol nitrate burden. The concentration enhancements are not uniformly distributed, but follow the regions of maximum emissions, and further downwind transport.

Besides the well known impacts of lightning on O_3, also the impact on the chemical oxidation capacity of the atmosphere is highly important for the upper tropospheric aerosol load. Because of a decrease of the oxidation potential (as represented by an increase in the methane lifetime), the sulphate formation via the gas phase reaction pathway is reduced in case of neglecting LNO_x emissions. Hence new particle formation is suppressed, efficiently modifying the small part of the aerosol size distribution. In addition to the condensation of nitrate on the aerosol particles, the combination of a reduced particle number and the coagulation of the particles, substantial effects on the particle size distribution in the upper troposphere are simulated.

The changes in aerosol size, chemical composition and number concentrations have implications on climate via both aerosol-radiation and aerosol-cloud interactions. Lightning and its consequences (nitrate formation, size distribution changes) causes mostly an increase in the total aerosol extinction with pronounced increase maxima in the upper troposphere. On the other hand, both liquid and ice phase cloud optical properties are modified by the LNO_x emissions, represented by e.g. effective droplet and ice crystal size. However, in contrast to the nitrate concentration increases the cloud effects resulting from lightning are ambiguous.

The resulting shortwave flux perturbations caused by LNO_x emissions are quantified to be ~ -100 mW/m^2. The resulting effect is caused mostly by the aerosol-cloud interactions, whereas the direct aerosol-radiation interactions are of secondary importance. However, an uncertainty range of

Atmos. Chem. Phys. Discuss., doi:10.5194/acp-2016-426, 2016
Manuscript under review for journal Atmos. Chem. Phys.
Published: 27 June 2016

Atmospheric Chemistry and Physics Discussions

almost ~ 50 mW/m^2 has to be assumed due to large internal variability and uncertainties in the process description (mostly in the aerosol-cloud interactions).

Nevertheless, an increase in lightning activity in the future or impacts of a more efficient transformation of the LNO_x emissions into nitrate under future climate conditions might have a non-negligible impact on the radiation balance of the atmosphere. On the other hand, aerosol nitrate formed from lightning offers further possibilities to address the feedback and (potentially compensating) impacts of combined chemistry-aerosol-climate interactions.

Acknowledgements. Parts of this research were conducted using the supercomputer Mogon and advisory services offered by Johannes Gutenberg University Mainz (www.hpc.uni-mainz.de), which is a member of the AHRP and the Gauss Alliance e.V. The authors gratefully acknowledge the computing time granted on the supercomputer Mogon at Johannes Gutenberg University Mainz (www.hpc.uni-mainz.de).

The author wishes to acknowledge use of the PARAVIEW program by the Sandia National Laboratories. Sandia is a multiprogram laboratory operated by Sandia Corporation, a Lockheed Martin Company, for the United States Department of Energy's National Nuclear Security Administration under contract DE-AC04-94AL85000.

The author wishes to acknowledge use of the Ferret program for analysis and graphics in this paper. Ferret is a product of NOAA's Pacific Marine Environmental Laboratory; further information is available at http://ferret.pmel.noaa.gov/Ferret/.

Furthermore, the author thanks all MESSy developers and users for support; further information can be found at http://www.messy-interface.org.

Atmos. Chem. Phys. Discuss., doi:10.5194/acp-2016-426, 2016
Manuscript under review for journal Atmos. Chem. Phys.
Published: 27 June 2016

Atmospheric Chemistry and Physics Discussions

References

Abdul-Razzak, H. and Ghan, S.: A parameterization of aerosol activation: 2. Multiple aerosol types, Journal of Geophysical Research: Atmospheres, 105, 6837–6844, 2000.

Adams, P. J., Seinfeld, J. H., Koch, D., Mickley, L., and Jacob, D.: General circulation model assessment of direct radiative forcing by the sulfate-nitrate-ammonium-water inorganic aerosol system, Journal of Geophysical Research: Atmospheres, 106, 1097–1111, 2001.

Albrecht, B. A.: Aerosols, Cloud Microphysics, and Fractional Cloudiness, Science, 245, 1227–1230, 1989.

Banerjee, A., Archibald, A. T., Maycock, A. C., Telford, P., Abraham, N. L., Yang, X., Braesicke, P., and Pyle, J. A.: Lightning NO_x, a key chemistry–climate interaction: impacts of future climate change and consequences for tropospheric oxidising capacity, Atmospheric Chemistry and Physics, 14, 9871–9881, doi:10.5194/acp-14-9871-2014, 2014.

Bauer, S. E., Koch, D., Unger, N., Metzger, S. M., Shindell, D. T., and Streets, D. G.: Nitrate aerosols today and in 2030: a global simulation including aerosols and tropospheric ozone, Atmospheric Chemistry and Physics, 7, 5043–5059, 2007.

Bellouin, N., Rae, J., Jones, A., Johnson, C., Haywood, J., and Boucher, O.: Aerosol forcing in the Climate Model Intercomparison Project (CMIP5) simulations by HadGEM2-ES and the role of ammonium nitrate, Journal of Geophysical Research: Atmospheres, 116, n/a–n/a, 2011.

Chang, D. Y., Tost, H., Steil, B., and Lelieveld, J.: Aerosol–cloud interactions studied with the chemistry-climate model EMAC, Atmospheric Chemistry and Physics Discussions, 14, 21 975–22 043, 2014.

de Meij, A., Pozzer, A., Pringle, K. J., Tost, H., and Lelieveld, J.: EMAC model evaluation and analysis of atmospheric aerosol properties and distribution with a focus on the Mediterranean region, Atmospheric Research, 114–115, 38 – 69, doi:10.1016/j.atmosres.2012.05.014, 2012.

Dentener, F., Kinne, S., Bond, T., Boucher, O., Cofala, J., Generoso, S., Ginoux, P., Gong, S., Hoelzemann, J. J., Ito, A., Marelli, L., Penner, J. E., Putaud, J.-P., Textor, C., Schulz, M., van der Werf, G. R., and Wilson, J.: Emissions of primary aerosol and precursor gases in the years 2000 and 1750 prescribed data-sets for AeroCom, Atmospheric Chemistry and Physics, 6, 4321–4344, doi:10.5194/acp-6-4321-2006, 2006.

Dietmüller, S., Jöckel, P., Tost, H., Kunze, M., Gellhorn, C., Brinkop, S., Frömming, C., Ponater, M., Steil, B., Lauer, A., and Hendricks, J.: A new radiation infrastructure for the Modular Earth Submodel System (MESSy, based on version 2.51), Geoscientific Model Development Discussions, 2016, 1–21, doi:10.5194/gmd-2015-277, 2016.

Fountoukis, C. and Nenes, A.: ISORROPIA II: a computationally efficient thermodynamic equilibrium model for K^+, Ca^{2+}, Mg^{2+}, $NH_4{}^+$, Na^+, $SO_4{}^{2-}$, $NO_3{}^-$, Cl^-, H_2O aerosols, Atmospheric Chemistry and Physics, 7, 4639–4659, doi:10.5194/acp-7-4639-2007, 2007.

Grewe, V.: Impact of climate variability on tropospheric ozone, Science of The Total Environment, 374, 167–181, doi:http://dx.doi.org/10.1016/j.scitotenv.2007.01.032, 2007.

IPCC: Climate Change 2013: The Physical Science Basis. Contribution of Working Group I to the Fifth Assessment Report of the Intergovernmental Panel on Climate Change, Cambridge University Press, Cambridge, United Kingdom and New York, NY, USA, doi:10.1017/CBO9781107415324, www.climatechange2013.org, 2013.

Atmos. Chem. Phys. Discuss., doi:10.5194/acp-2016-426, 2016
Manuscript under review for journal Atmos. Chem. Phys.
Published: 27 June 2016

Jacobson, M. Z.: Global direct radiative forcing due to multicomponent anthropogenic and natural aerosols, Journal of Geophysical Research: Atmospheres, 106, 1551–1568, 2001.

Jaegle, L., Steinberger, L., Martin, R. V., and Chance, K.: Global partitioning of NOx sources using satellite observations: Relative roles of fossil fuel combustion, biomass burning and soil emissions, Faraday Discuss., 130, 407–423, 2005.

Jöckel, P., Sander, R., Kerkweg, A., Tost, H., and Lelieveld, J.: Technical Note: The Modular Earth Submodel System (MESSy) - a new approach towards Earth System Modeling, Atmos. Chem. Phys., 5, 433–444, 2005.

Jöckel, P., Kerkweg, A., Pozzer, A., Sander, R., Tost, H., Riede, H., Baumgaertner, A., Gromov, S., and Kern, B.: Development cycle 2 of the Modular Earth Submodel System (MESSy2), Geoscientific Model Development, 3, 717–752, doi:10.5194/gmd-3-717-2010, 2010.

Kärcher, B., Hendricks, J., and Lohmann, U.: Physically based parameterization of cirrus cloud formation for use in global atmospheric models, J. Geophys. Res., 111, D01 206, doi:10.1029/2005JD006219, 2006.

Kerkweg, A., Buchholz, J., Ganzeveld, L., Pozzer, A., Tost, H., and Jöckel, P.: Technical Note: An implementation of the dry removal processes DRY DEPosition and SEDImentation in the Modular Earth Submodel System (MESSy), Atmos. Chem. Phys., 6, 4617–4632, 2006a.

Kerkweg, A., Sander, R., Tost, H., and Jöckel, P.: Technical Note: Implementation of prescribed (OFFLEM), calculated (ONLEM), and pseudo-emissions (TNUDGE) of chemical species in the Modular Earth Submodel System (MESSy), Atmos. Chem. Phys., 6, 3603–3609, 2006b.

Labrador, L. J., v. Kuhlmann, R., and Lawrence, M. G.: Strong sensitivity of the global mean OH concentration and the tropospheric oxidizing efficiency to the source of NO_x from lightning, Geophys. Res. Lett., 31, L06 102, doi:10.1029/2003GL019229, 2004.

Labrador, L. J., v. Kuhlmann, R., and Lawrence, M. G.: The effects of lightning-produced NO_x and its vertical distribution on atmospheric chemistry: sensitivity simulations with MATCH-MPIC, Atmos. Chem. Phys., 5, 1815–1834, 2005.

Lamarque, J.-F., Bond, T. C., Eyring, V., Granier, C., Heil, A., Klimont, Z., Lee, D., Liousse, C., Mieville, A., Owen, B., Schultz, M. G., Shindell, D., Smith, S. J., Stehfest, E., Van Aardenne, J., Cooper, O. R., Kainuma, M., Mahowald, N., McConnell, J. R., Naik, V., Riahi, K., and van Vuuren, D. P.: Historical (1850–2000) gridded anthropogenic and biomass burning emissions of reactive gases and aerosols: methodology and application, Atmospheric Chemistry and Physics, 10, 7017–7039, doi:10.5194/acp-10-7017-2010, 2010.

Lohmann, U. and Hoose, C.: Sensitivity studies of different aerosol indirect effects in mixed-phase clouds, Atmospheric Chemistry and Physics, 9, 8917–8934, 2009.

Lohmann, U., Rotstayn, L., Storelvmo, T., Jones, A., Menon, S., Quaas, J., Ekman, A. M. L., Koch, D., and Ruedy, R.: Total aerosol effect: radiative forcing or radiative flux perturbation?, Atmospheric Chemistry and Physics, 10, 3235–3246, 2010.

Makkonen, R., Romakkaniemi, S., Kokkola, H., Stier, P., Räisänen, P., Rast, S., Feichter, J., Kulmala, M., and Laaksonen, A.: Brightening of the global cloud field by nitric acid and the associated radiative forcing, Atmospheric Chemistry and Physics, 12, 7625–7633, 2012.

Mao, K., Ma, Y., Xia, L., Chen, W. Y., Shen, X., He, T., and Xu, T.: Global aerosol change in the last decade: An analysis based on {MODIS} data, Atmospheric Environment, 94, 680 – 686, 2014.

Martin, R. V., Jacob, D. J., Logan, J. A., Bey, I., Yantosca, R. M., Staudt, A. C., Li, Q., Fiore, A. M., Duncan, B. N., Liu, H., Ginoux, P., and Thouret, V.: Interpretation of TOMS observations of tropical tropospheric ozone with a global model and in situ observations, Journal of Geophysical Research: Atmospheres, 107, ACH 4–1–ACH 4–27, doi:10.1029/2001JD001480, 4351, 2002.

Mayer, B. and Kylling, A.: Technical note: The libRadtran software package for radiative transfer calculations - description and examples of use, Atmospheric Chemistry and Physics, 5, 1855–1877, 2005.

Petters, M. D. and Kreidenweis, S. M.: A single parameter representation of hygroscopic growth and cloud condensation nucleus activity, Atmospheric Chemistry and Physics, 7, 1961–1971, doi:10.5194/acp-7-1961-2007, 2007.

Pickering, K. E., Wang, Y., Tao, W.-K., Price, C., and Müller, J.-F.: Vertical distribution of lightning NO_x for use in regional and chemical transport models, J. Geophys. Res., 103, 31 203–31 216, 1998.

Pozzer, A., de Meij, A., Pringle, K. J., Tost, H., Doering, U. M., van Aardenne, J., and Lelieveld, J.: Distributions and regional budgets of aerosols and their precursors simulated with the EMAC chemistry-climate model, Atmospheric Chemistry and Physics, 12, 961–987, doi:10.5194/acp-12-961-2012, 2012.

Price, C. and Rind, D.: A simple Lightning Parametrization for Calculating Global Lightning Distributions, J. Geophys. Res., 97, 9919–9933, 1992.

Pringle, K. J., Tost, H., Metzger, S., Steil, B., Giannadaki, D., Nenes, A., Fountoukis, C., Stier, P., Vignati, E., and Lelieveld, J.: Description and evaluation of GMXe: a new aerosol submodel for global simulations (v1), Geoscientific Model Development, 3, 391–412, doi:10.5194/gmd-3-391-2010, 2010.

Roeckner, E., Bäuml, G., Bonaventura, L., Brokopf, R., Esch, M., Giorgetta, M., Hagemann, S., Kirchner, I., Kornblue, L., Manzini, E., Rhodin, A., Schleese, U., Schulzweida, U., and Tompkins, A.: The atmospheric general circulation model ECHAM5: Part 1, Tech. Rep. 349, Max-Planck-Institut für Meteorologie, 2003.

Roeckner, E., Brokopf, R., Esch, M., Giogetta, M., Hagemann, S., Kornblueh, L., Manzini, E., Schleese, U., and Schulzweida, U.: Sensitivity of simulated climate to horizontal and vertical resolution in the ECHAM5 atmosphere model, J. Clim., 19, 3771–3791, 2006.

Sander, R., Baumgaertner, A., Gromov, S., Harder, H., Jöckel, P., Kerkweg, A., Kubistin, D., Regelin, E., Riede, H., Sandu, A., Taraborrelli, D., Tost, H., and Xie, Z.-Q.: The atmospheric chemistry box model CAABA/MECCA-3.0, Geoscientific Model Development, 4, 373–380, doi:10.5194/gmd-4-373-2011, 2011.

Schumann, U. and Huntrieser, H.: The global lightning-induced nitrogen oxides source, Atmos. Chem. Phys., 7, 3823–3907, doi:10.5194/acp-7-3823-2007, 2007.

Steinkamp, J. and Lawrence, M. G.: Improvement and evaluation of simulated global biogenic soil NO emissions in an AC-GCM, Atmospheric Chemistry and Physics, 11, 6063–6082, 2011.

Stelson, A., Friedlander, S., and Seinfeld, J.: A note on the equilibrium relationship between ammonia and nitric acid and particulate ammonium nitrate, Atmospheric Environment (1967), 13, 369 – 371, 1979.

Tanre, D., Geleyn, J.-F., and Slingo, J. M.: Aerosols and Their Climatic Effects, chap. First results of the introduction of an advanced aerosol-radiation interaction in the ecmwf low resolution global model, A. Deepak, Hampton, Va., 1984.

Tiedtke, M.: A Comprehensive Mass Flux Scheme for Cumulus Parametrization in Large-Scale Models, Mon. Weather Rev., 117, 1779–1800, 1989.

Atmos. Chem. Phys. Discuss., doi:10.5194/acp-2016-426, 2016
Manuscript under review for journal Atmos. Chem. Phys.
Published: 27 June 2016

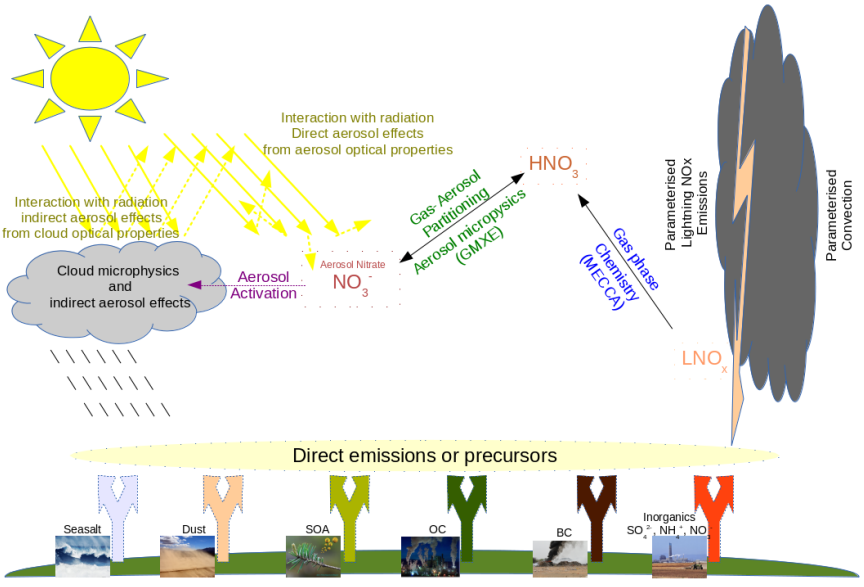

Figure 1. Sketch of the simulated processes from the emission of NO_x molecules by lightning over gas phase conversion to HNO_3, gas aerosol partitioning to particulate NO_3^- and implications for the direct and indirect aerosol effects.

Tost, H. and Pringle, K. J.: Improvements of organic aerosol representations and their effects in large-scale atmospheric models, Atmospheric Chemistry and Physics, 12, 8687–8709, doi:10.5194/acp-12-8687-2012, 2012.

Tost, H., Jöckel, P., Kerkweg, A., Sander, R., and Lelieveld, J.: Technical Note: A new comprehensive SCAVenging submodel for global atmospheric chemistry modelling, Atmos. Chem. Phys., 6, 565–574, 2006.

Tost, H., Jöckel, P., and Lelieveld, J.: Lightning and convection parameterisations - uncertainties in global modelling, Atmos. Chem. Phys., 7, 4553–4568, 2007.

Twomey, S.: The Influence of Pollution on the Shortwave Albedo of Clouds, Journal of the Atmospheric Sciences, 34, 1149–1152, doi:10.1175/1520-0469(1977)034<1149:TIOPOT>2.0.CO;2, 1977.

van der Werf, G. R., Randerson, J. T., Giglio, L., Collatz, G. J., Mu, M., Kasibhatla, P. S., Morton, D. C., DeFries, R. S., Jin, Y., and van Leeuwen, T. T.: Global fire emissions and the contribution of deforestation, savanna, forest, agricultural, and peat fires (1997–2009), Atmospheric Chemistry and Physics, 10, 11 707–11 735, doi:10.5194/acp-10-11707-2010, 2010.

Xu, L. and Penner, J. E.: Global simulations of nitrate and ammonium aerosols and their radiative effects, Atmospheric Chemistry and Physics, 12, 9479–9504, 2012.

Atmos. Chem. Phys. Discuss., doi:10.5194/acp-2016-426, 2016
Manuscript under review for journal Atmos. Chem. Phys.
Published: 27 June 2016

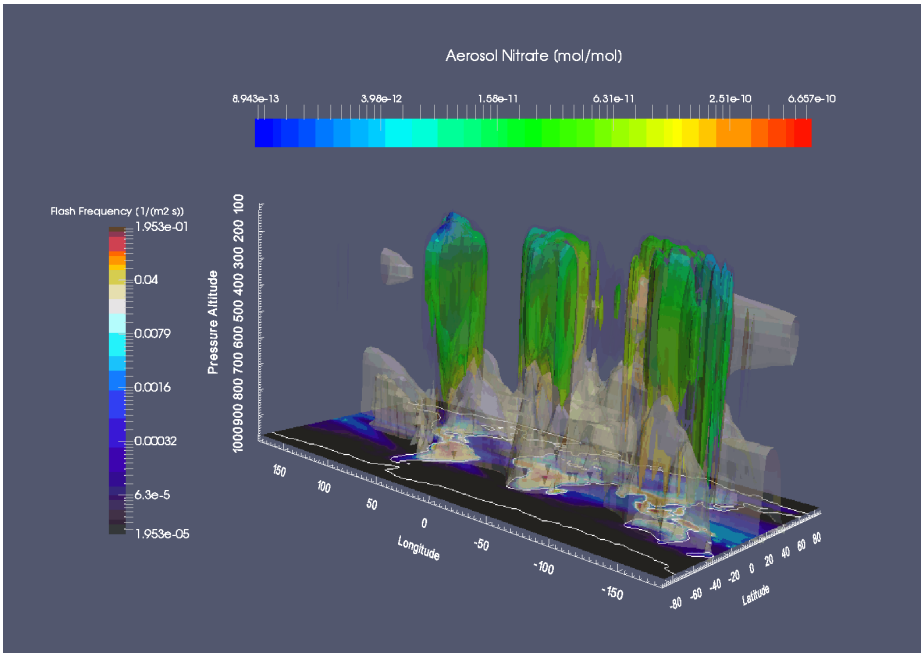

Figure 2. 3D visualisation of LNO_x emissions (coloured isosurface of $1 \cdot 10^{-16}$ kg/(m^{3}s) and darker shaded isosurface of $3 \cdot 10^{-16}$ kg/(m^{3}s)) and the total aerosol nitrate mixing ratios (grey isosurface of 0.1 ppb_v). Additionally, the mean flash rate in 1/s is depicted by the 2D slice at the bottom. Note the logarithmic scaling of both colour bars.

Atmos. Chem. Phys. Discuss., doi:10.5194/acp-2016-426, 2016
Manuscript under review for journal Atmos. Chem. Phys.
Published: 27 June 2016

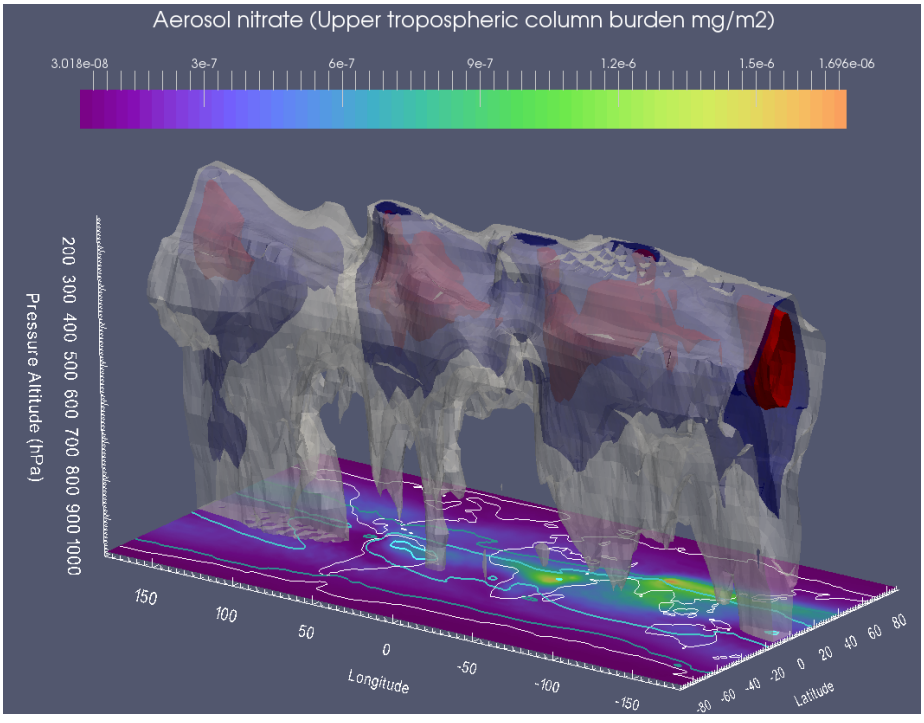

Figure 3. 3D visualisation of the relative differences in tropospheric aerosol nitrate mixing ratios between the simulations with and without LNO_x emissions to the simulation including LNO_x emissions. The white isosurface depicts a relative difference of 30%, the blue isosurface of 45%, and the red isosurface of 60%. Additionally, the upper tropospheric aerosol nitrate column burden (in mg/m^2) between 500 hPa and the tropopause is depicted by the coloured panel at the bottom of the graph. The turquoise contour lines depict relative differences of 20%, 40% and 60% difference in this column burden between the two simulations.

Atmos. Chem. Phys. Discuss., doi:10.5194/acp-2016-426, 2016
Manuscript under review for journal Atmos. Chem. Phys.
Published: 27 June 2016

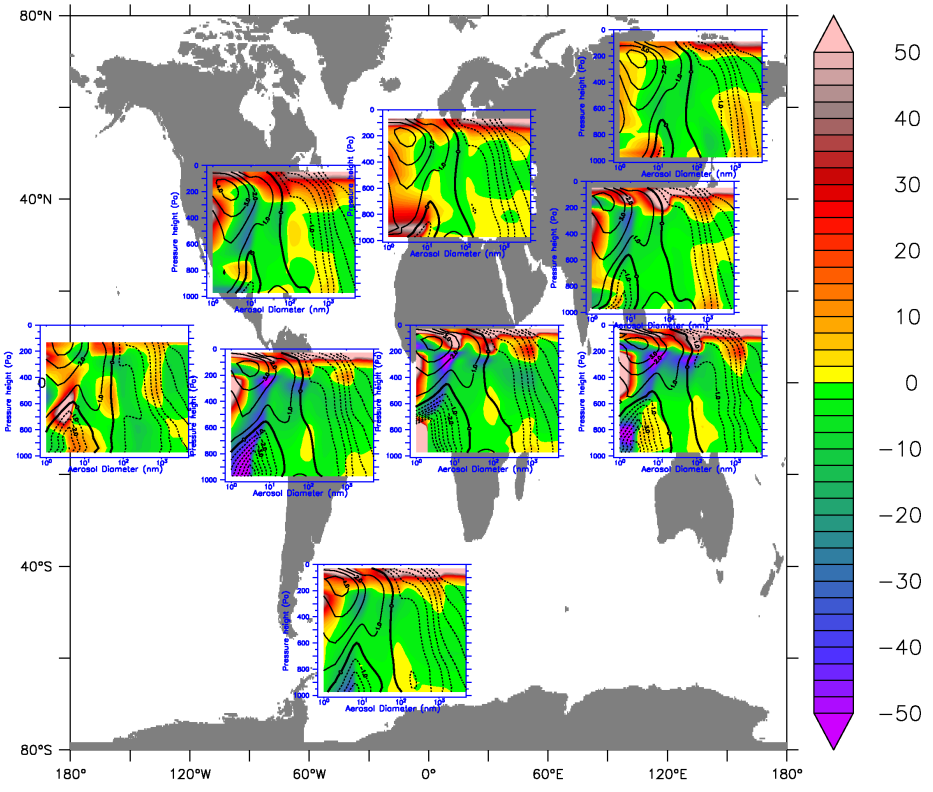

Figure 4. Map of vertically resolved percentage differences (including LNO_x emissions as the reference case) in the aerosol size distributions as spatial and regional average (for the respective regions). Overlayed are the contours of the absolute values of the size distributions, i.e. the absolute particle numbers calculated from the overlaying of the individual modes, determined from the spatial and temporal mean in particles/cm^3. The figure depicts the present day conditions. The respective regions are: Central Pacific (150W:110W, 20S:0), Amazonia (80W:35W, 20S:10N), Eastern US (100W:75W, 30N:45N), South Atlantic (50W:10W, 80S:60S), Central Africa (5E:45E, 10S:10N), Europe (10W:25E, 40N:60N), Indonesia (95E:155E, 12S:10N), East Asia (105E:125E, 20N:42N), Siberia (60E:100E, 50N:70N).

Atmos. Chem. Phys. Discuss., doi:10.5194/acp-2016-426, 2016
Manuscript under review for journal Atmos. Chem. Phys.
Published: 27 June 2016

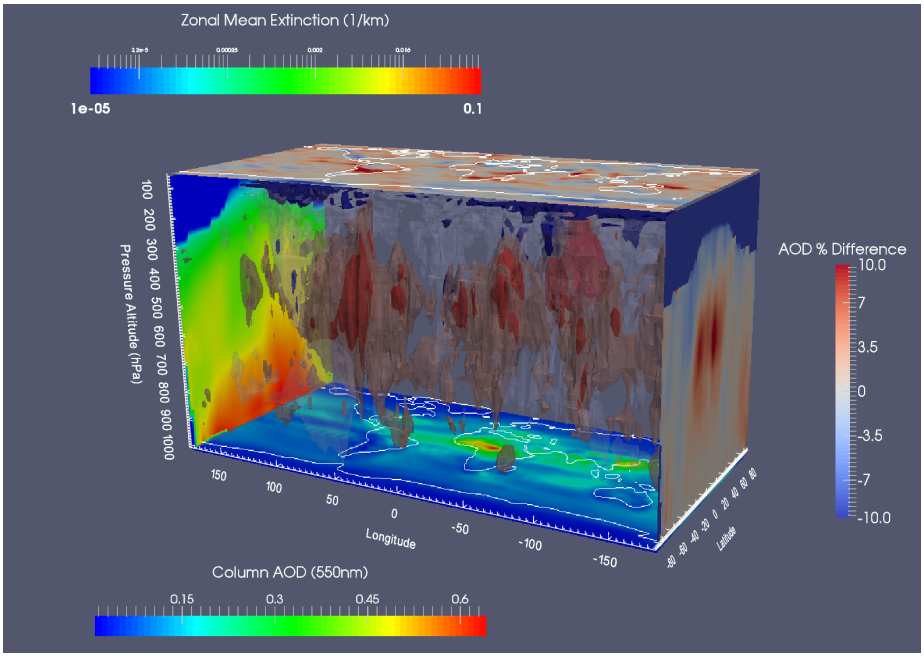

Figure 5. 3D visualisation of aerosol extinction and the influence of LNO_x emissions. The floor shows a map of the vertically integrated column AOD (at 550 nm) when lightning emissions are included. The ceiling depicts the relative differences of the integrated column AOD between the simulation with lightning emissions minus the simulation without lightning LNO_x, with the full setup serving as reference. The back panel displays the zonal average aerosol extinction (in 1/km at 550 nm) of the full simulations (Please, note the logarithmic scale.). Additionally, the front panel depicts again relative percentage differences due NO_x emissions from lightning. The 3D isosurfaces in the center of the box represent the $+10\%$ (pale red) and $+20\%$ (dark red) of the enhanced extinction due to active LNO_x emissions, whereas the -10% (pale blue) and -20% (dark blue) isosurfaces mark regions, in which the emissions result in a reduction of the extinction.

Atmos. Chem. Phys. Discuss., doi:10.5194/acp-2016-426, 2016
Manuscript under review for journal Atmos. Chem. Phys.
Published: 27 June 2016

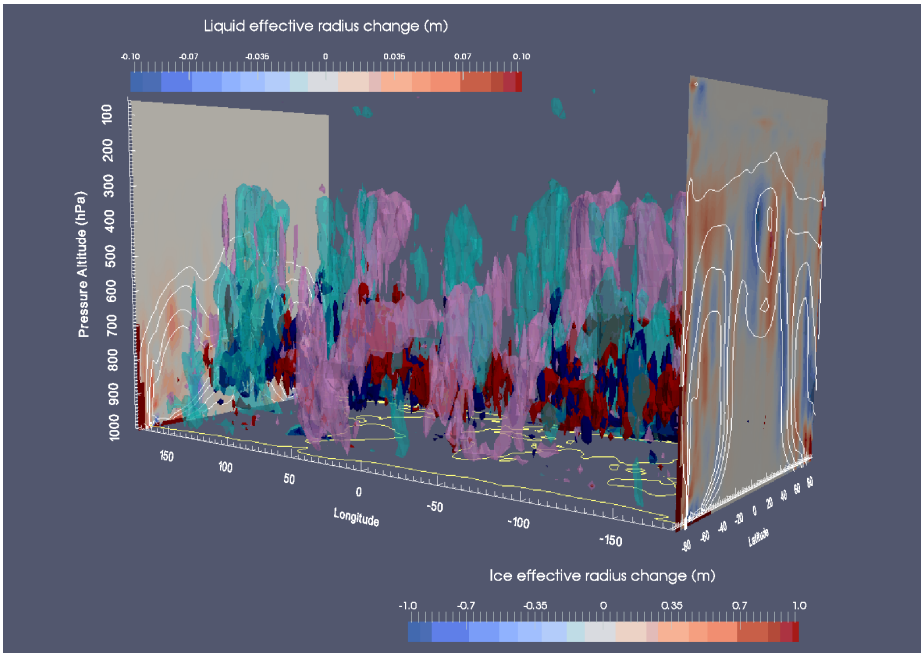

Figure 6. Visualisation of changes in the effective radius of liquid water droplets and ice crystals. The back panel displays the zonal average liquid droplet effect radius (white contours) and the absolute changes due to the LNO_x emissions. The front panel depicts similarly the ice crystal effective size (white contours) and the absolute change due to the lightning emissions. Additionally, the isosurfaces represent the regions for substantial absolute changes for the effective radius for water droplets (blue negative, red positive) and effective ice crystal size (turquoise for negative and purple for positive) due the LNO_x emissions.

Atmos. Chem. Phys. Discuss., doi:10.5194/acp-2016-426, 2016
Manuscript under review for journal Atmos. Chem. Phys.
Published: 27 June 2016

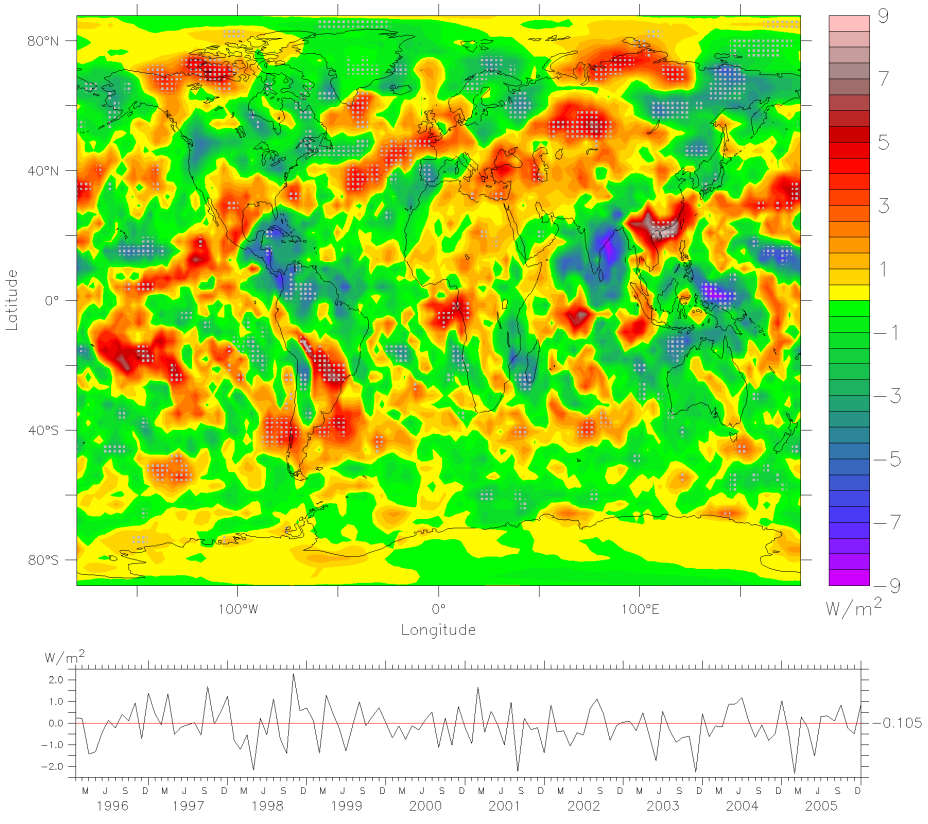

Figure 7. Absolute changes in the shortwave all-sky fluxes at the top of the atmosphere. The upper panel depicts the long term time average of the difference in the simulation with LNO_x emissions minus the fluxes without lightning emissions. The hatches mark regions with a statistical significant signal (compared to the internal interannual variability). The bottom panel depicts the time series of the monthly mean global mean differences with the red line marking a 0 W/m^2 change.

Atmos. Chem. Phys. Discuss., doi:10.5194/acp-2016-426, 2016
Manuscript under review for journal Atmos. Chem. Phys.
Published: 27 June 2016

Atmospheric Chemistry and Physics Discussions

Table 1. Tropospheric and upper tropospheric burden in the ARG simulation of the important highly oxidised nitrogen species, i.e. gaseous HNO_3, gaseous N_2O_5, aerosol NO_3^- and the sum of those three compounds. All values are given in Gg N (except for the relative differences which are provided in %) and are globally and vertically integrated over the whole and the upper troposphere (500hPa up to the tropopause).

	HNO_3	N_2O_5	NO_3^-	Total N(V+)
Present day				
Absolute values (with LNO_x emissions):				
Tropospheric Column burden	403	8.0	143	554
UT Column burden	174	5.0	27.8	207
Absolute differences due to LNO_x emissions:				
Tropospheric Column burden	162	3.9	20.0	186
UT Column burden	107	3.5	9.0	119
Relative differences in (%) due to LNO_x emissions:				
Tropospheric Column burden	40.1	48.4	14.0	33.5
UT Column burden	61.3	70.3	32.3	57.7
Preindustrial conditions				
Absolute values (with LNO_x emissions):				
Tropospheric Column burden	238	4.5	67.8	310
UT Column burden	143	4.1	15.0	161
Absolute differences due to LNO_x emissions:				
Tropospheric Column burden	158	3.7	25.8	188
UT Column burden	110	3.5	8.1	121
Relative differences in (%) due to LNO_x emissions:				
Tropospheric Column burden	66.6	82.6	38.1	60.6
UT Column burden	76.9	86.0	54.3	75.1

Atmos. Chem. Phys. Discuss., doi:10.5194/acp-2016-426, 2016
Manuscript under review for journal Atmos. Chem. Phys.
Published: 27 June 2016

Atmospheric Chemistry and Physics Discussions

Table 2. CH_4 tropospheric and upper tropospheric (500 hPa to tropopause) lifetime and absolute increase due to the neglect of LNO_x emissions.

	CH_4 lifetime [years]	Increase of the CH_4 lifetime [years]
Present day		
troposphere	7.4	1.7
UT only	14.0	9.7
Preindustrial conditions		
troposphere	8.9	1.9
UT only	14.1	13.2